Available online at www.sciencedirect.com
SCIENCE DIRECT®
Journal of Photochemistry and Photobiology A: Chemistry 168 (2004) 23–30
Journal of Photochemistry and Photobiology A:Chemistry
www.elsevier.com/locate/jphotochem

Heterogeneous photocatalytic degradation of the anthraquinonic dye, Acid Blue 25 (AB25): a kinetic approach

I. Bouzaida [a,b], C. Ferronato [a], J.M. Chovelon [a,*], M.E. Rammah [b], J.M. Herrmann [a]

[a] *Laboratoire d'Application de la Chimie à l'Environnement (LACE), UMR-CNRS 5634, Université Claude Bernard Lyon 1, 43 Bd du 11 novembre 1918, 69622 Villeurbanne Cedex, France*

[b] *Laboratoire de Physique et Chimie des Interfaces, Faculté des Sciences de Monastir, Université du Centre, Avenue de l'Environnement, 5019 Monastir, Tunisia*

Received 13 February 2004; received in revised form 7 May 2004; accepted 11 May 2004
Available online 6 July 2004

Abstract

The photocatalytic degradation of the anthraquinonic dye, Acid Blue 25 was investigated in aqueous solutions containing TiO_2 suspension as photocatalyst. The influence of parameters such as adsorption of the dye onto TiO_2, pH, temperature, catalyst concentration and photon flux were studied. Results showed that adsorption played an important role in the control of the photocatalytic degradation rate and an optimal TiO_2 concentration of $2.6\,g\,L^{-1}$ was determined. By comparing the disappearance of AB25 followed by HPLC–DAD (high performance liquid chromatography–diode array detector) and the bleaching of the solution followed by UV-Vis spectrometry (wavelength of analysis = 600 nm), two different kinetics were found proving that some of the intermediate products were still colored. This was confirmed using HPLC–DAD and HPLC–MS (high performance liquid chromatography—mass spectrometry) analysis.
© 2004 Elsevier B.V. All rights reserved.

Keywords: Photocatalysis; Titania; Dye; Acid Blue 25; Decolorization; Total degradation

1. Introduction

Dyes can be discharged to the aquatic environment from three major sources: (a) from dye manufacturers, (b) from dye users (i.e. textile, paper, plastic industries, etc.) and (c) from diffuse or household discharges as a result of leaching of dye from manufactured products. As a consequence, dyes is becoming a major source of environmental contamination. As the international environmental standards are becoming more stringent, many research studies have been focussed on the treatments of colored wastewater. However, because of the complexity and the variety of dyestuffs employed in the dyeing processes, it has become rather difficult to find an unique treatment procedure that entirely covers the effective elimination of all types of dyes. Particularly, biochemical oxidation suffers from significant limitations since most dyestuffs commercially available have been intentionally designed to resist aerobic microbial degradation.

Heterogeneous photocatalysis appears as an emerging and interesting technology for the degradation of organic pollutants such as dyes as it can utilize sunlight as a source of energy, which is free and inexhaustible [1–8]. Unfortunately, only 5% of the solar energy reaching the earth's surface can be absorbed by a classical photocatalysts such as titania.

However, despite this low percentage of UV light absorbable by TiO_2, it is possible to perform solar detoxification of wastewater contaminated by dyes. In particular, countries such as Tunisia for which dying processes represent an intense activity in textile industries, could treat efficiently and at low cost, wastewater contaminated by dyes since sunlight is very abundant.

In the present work the photocatalytic degradation in aqueous solution of the anthraquinonic dye Acid Blue 25 (AB25) was investigated. Anthraquinonic dyes represent the second most important class of commercial dyes after azo-compounds and are mainly used for dying wool, polyamide and leather.

The structure of Acid Blue 25 is shown in Fig. 1. To optimize the kinetic of the degradation process, several parameters such as adsorption, pH, temperature, catalyst concentrations and photon flux were studied.

* Corresponding author. Tel.: +33-472432638; fax: +33-472448438.
E-mail address: chovelon@univ-lyonl.fr (J.M. Chovelon).

1010-6030/$ – see front matter © 2004 Elsevier B.V. All rights reserved.
doi:10.1016/j.jphotochem.2004.05.008

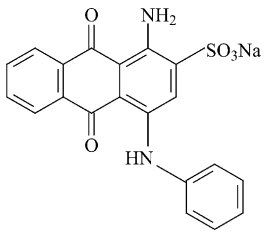

Fig. 1. Structure of Acid Blue 25.

2. Material and procedure

2.1. Materials and reagents

Acid Blue 25 [1-amino-9,10-dihydro-9,10-dioxo-4-(phenylamino)-2-anthracenesulfonic acid, monosodium salt] (dye content 45%) was purchased from Aldrich (Saint Quentin en Fallavier, France) and was used as received. The remaining products do not absorb in the spectral range 200–900 nm. Acetonitrile for HPLC (high performance liquid chromatography) analysis was obtained from Fisher Chemical (Loughborough, Leics., UK). Deionized water was produced by a Milli-Q system and used systematically. The photocatalyst was TiO_2 Degussa P-25, mainly anatase (80%), with a specific surface area of $50\,m^2\,g^{-1}$ and a mean particle size of 30 nm.

2.2. Photoreactor and light source

The irradiation experiments were carried out in a 60 mL Pyrex cylindrical flask, open to air, with an optical window (at the bottom) of about 3 cm in diameter and a thermostated water-circulating jacket of about 6 cm diameter. It was mounted at a distance of 6 cm from the top of the lamp assembly, which consisted of a horizontal Philips HPK 125 W mean pressure mercury lamp (the wavelength maximum of the light source was 365 nm). The light intensity could be reduced by intercaling metallic calibrated grids between the lamp and the reactor. The light intensity received by the solutions was evaluated using uranyle oxalate as actinometer. It was found that the number of the photons potentially absorbable by TiO_2 in the irradiation cell could vary from 4×10^{15} to 1.3×10^{17} photons per second. For all experiments, the suspensions were magnetically stirred without any permanent air bubbling. In these conditions, the oxygen dissolved in water following Henry's law is sufficient to ensure a constant oxygen coverage of the surface of titania [6].

2.3. Procedure

A volume of 25 mL of aqueous solution of AB25 was introduced in the reactor. Adsorption and degradation were carried out at different temperatures (25, 30, 40, 50 and 60 °C) and at different pHs (5–8). The pH was adjusted either by using NaOH or HNO_3.

To determine the adsorption constants, different concentrations of AB25 were used. Before analysis, aliquots of the aqueous suspensions were collected at selected time intervals and filtered through 0.45 PVDF filters (Millipore) to remove TiO_2 particles.

2.4. Analyses

The UV-Vis absorption spectra were recorded using a double-beam UVIKON spectrophotometer (Kontron Instruments).

The HPLC–diode array detector (HPLC-DAD) analyses were performed using a Shimadzu HPLC system. The column was a Kromasil C_4, 5 μm (250 mm × 4 mm); the flow rate was $1\,mL\,min^{-1}$ and the injection volume was 20 μL. The mobile phase was acetonitrile (A) and water (B), whose pH was adjusted to 4.5 using a mixture of acetic acid and ammonium acetate. The isocratic elution conditions were 42% (A) + 58% (B) and the retention time was 10.2 min for AB25. The wavelength for detection was 600 nm which was chosen at the maximal absorption value for AB25. Total organic carbon (TOC) was determined using a Shimadzu TOC analyzer (model 5050 A). The HPLC–mass spectrometry (HPLC–MS) identification of photoproducts was performed using a Hewlet-Packard HP 1100 series LC–MSD (mass spectrometry detector). The column was a Uptishere C18 HDO, 3 μm (150 mm × 3 mm) and the mobile phase was acetonitrile (A) and water (B) whose pH was adjusted to 4.5 using a mixture of acetic acid and ammonium acetate. A gradient elution was used from 0 to 100% (A) in 25 min. The MS detection was performed with electrospray ionization (ESI) in negative mode.

3. Results and discussion

3.1. Preliminary adsorption in the dark

Since the degradation rate generally depends on the amount of adsorbed molecules, a series of experiments were carried out in the dark to study the adsorption of AB25 on TiO_2 surface. First of all, different concentrations of AB25 were used to study their adsorption isotherm ($T = 20\,°C$ and pH 6.6). Whatever the initial concentrations (from 24 to $168\,\mu mol\,L^{-1}$), it was found that an equilibrium adsorption of a Langmuirian type was reached in less than 15 min.

According to the Langmuir model the coverage θ varies as

$$\theta = \frac{Q_{ads}}{Q_{max}} = \frac{KC_{eq}}{1 + KC_{eq}} \quad (1)$$

where Q_{ads} is the number of adsorbed molecules at the adsorption equilibrium, Q_{max} the maximal adsorbable quantity, K the Langmuir adsorption constant of AB25 on TiO_2 and C_{eq} the concentration of AB25 at the adsorption equilibrium.

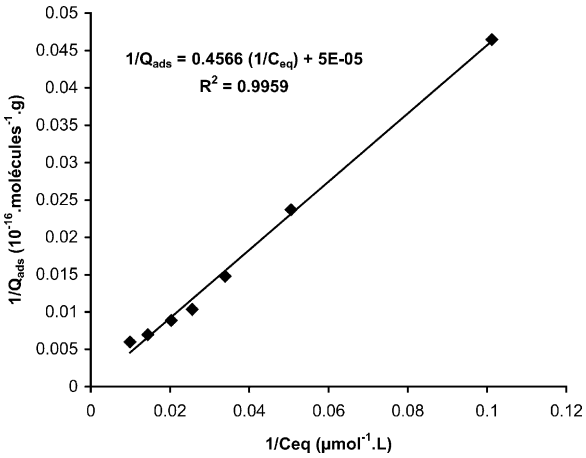

Fig. 2. Transformation of Langmuir isotherm: reciprocal of the quantity adsorbed as a function of reciprocal of equilibrium concentration (pH 6.6 and $T = 20\,^{\circ}C$).

Fig. 2 represents the linear transformation of Eq. (1) which is expressed by the following equation:

$$\frac{1}{Q_{ads}} = \frac{1}{Q_{max}} + \frac{1}{Q_{max} K C_{eq}} \quad (2)$$

In this curve, the ordinate at the origin is equal to the reciprocal of Q_{max}, whereas K can be calculated from the slope (slope $= 1/Q_{max}K$).

In Table 1, adsorption parameters (Q_{max} and K) for AB25 were reported, as well as the maximal coverage of TiO_2 determined by taking into account the maximum number of adsorption sites estimated to be equal to $5\,nm^{-2}$ [9,10]. It appears that the value of K is in agreement with that of other dyes which have an analogous structure [11]. For example, for alizarin S which is also an anthraquinonic dye, a value of $4180\,L\,mol^{-1}$ has been found [11] against a present value of $894\,L\,mol^{-1}$. Anyway, such a value has to be used carefully since a very slight variation in the calculation of the slope can give rise to a significant variation of K values.

Since real effluents to be treated can be at different temperatures (according to the seasons, the geographical sites, during the treatment itself, etc.) and at different pHs, comparative experiments were performed by varying these parameters.

Fig. 3 shows the variation of dyes adsorbed on TiO_2 ($\mu mol\,g^{-1}$) as a function of pH for a fixed temperature of $T = 30\,^{\circ}C$. It is shown that when the pH increases, a decrease of the amount of dye adsorbed on TiO_2 occurs. Such a result can be better understood taking into account both

Table 1
Adsorption characteristics of AB25 onto TiO_2

K ($L\,mol^{-1}$)	894
Q_{max} ($\mu mol\,g^{-1}$)	42.04
Q_{max} (molecules nm^{-2})	0.5064
θ_{max} (%)	10.13

K, Langmuir adsorption constant and Q_{max}, maximum quantities adsorbed.

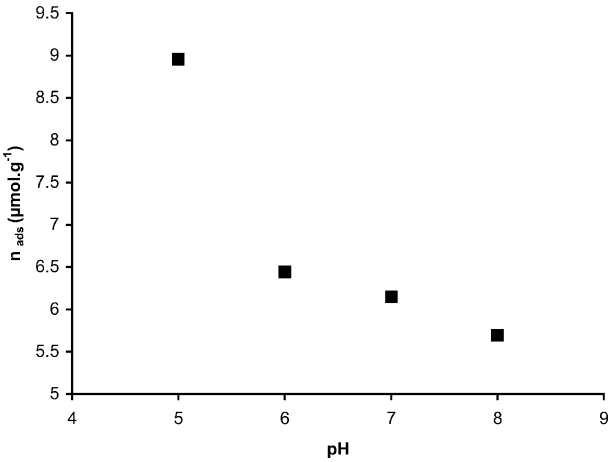

Fig. 3. Variation of dyes adsorbed on TiO_2 as a function of pH for a fixed temperature of $T = 30\,^{\circ}C$.

the surface state of titania and the ionization state of the dye. The point of zero charge (pH_{pzc}) of TiO_2 is known to be close to pH 6.8 which means that for pH's higher than 6.8, the surface becomes negatively charged according to the electrochemical equilibrium:

$$TiOH + OH^- \rightleftarrows H_2O + TiO^- \quad (3)$$

And at $pH < pH_{pzc}$, the surface of titania is positively charged according to

$$TiOH + H^+ \rightleftarrows Ti\text{–}OH_2{}^+ \quad (4)$$

On other hand AB25 is an anionic dye bearing an anionic sulfonate function (cf. Fig. 1). In this context, it is conceivable that at high pH values an electrostatic repulsion between TiO_2 and the dye occurs which leads to a decrease in the amount of dye adsorbed on TiO_2. In the following, a pH close to 6.6 was used.

Fig. 4 shows the variation of the dyes adsorbed on TiO_2 as a function of temperature for four different pHs (5–8). Whatever the pH chosen, a decrease of the amount of dye adsorbed is observed when temperature increases and such

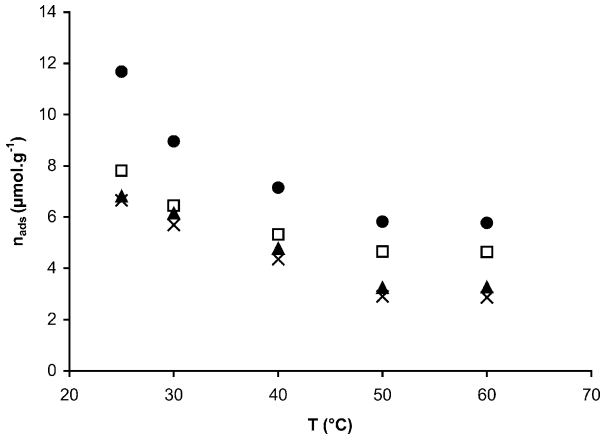

Fig. 4. Variation of dyes adsorbed on TiO_2 as a function of temperature for four different pH (●, pH = 5; □, pH = 6; ▲, pH = 7; ×, pH = 8).

Table 2
Values of enthalpy of adsorption (ΔH), activation energy (E_a) and true activation energy (E_t) given at different pH

pH	ΔH (kJ mol^{-1})	E_a (kJ mol^{-1})	E_t (kJ mol^{-1})
5	−21.3	−8.3	13.0
6	−21.3	−11.1	10.2
7	−23.7	−12.5	11.2
8	−26.0	Not calculated	Not calculated

a trend appears to be more pronounced for the lowest pH values. From these results, the enthalpy of adsorption (ΔH) at different pH have been calculated (cf. Table 2) using the linear transformation of the following equation.

$$Q_{ads} = (Q_{ads})_0 \exp\left[-\left(\frac{\Delta H}{RT}\right)\right] \quad (5)$$

The linear transformation of its equation expressed by $\ln(Q_{ads}) = (1/T)$ gives a straight line whose slope is equal to $-\Delta H/R$.

As expected, Table 2 shows that the adsorption reactions are exothermic and since all the values obtained whatever the pH remain small, it seems that molecules are only weakly adsorbed on the surface. Moreover, for pH lesser than the pH_{pzc}, similar values are obtained (≈ -21 kJ mol^{-1}), whereas, for pH higher than pH_{pzc}, values becomes more important since molecules have to overcome electrostatic repulsion between TiO_2 and the dye to be adsorbed.

3.2. Photocatalytic degradation of AB25

For the subsequent experiments, the dye solution was magnetically stirred in the dark during 30 min before irradiating the reactor to make sure that adsorption equilibrium was reached. During photocatalytic degradation, intermediates are formed and may interfere in the determination of kinetics because of competitive adsorption and degradation. Therefore, calculations were done for conversions smaller than 15%. During this interval of time, the influence of intermediates could be considered as negligible.

3.2.1. Kinetic studies

Fig. 5 shows both disappearance of AB25 and bleaching of the solution followed by HPLC–DAD and UV-Vis spectrometry, respectively (wavelength of analysis = 600 nm). Information obtained from both curves are different but complementary, since HPLC measures only AB25 disappearance, whereas spectrometry follows all the products absorbing at 600 nm (AB25 plus intermediates). From these curves, the half-reaction times were calculated by assuming an apparent first-order kinetic law as it will presented in the next section. 15 min ($k = 4.72 \times 10^{-2}$ min^{-1}) and 124 min ($k = 5.6 \times 10^{-3}$ min^{-1}) were obtained for disappearance of AB25 and for bleaching, respectively. As these results are not equivalent, we can conclude that some of the intermediate products were still colored. This was confirmed (i) by the photoproducts UV spectra (from HPLC–DAD) and (ii) by HPLC–MS analysis which allows us to tentatively identify the main photoproducts (cf. Table 3). Table 3 shows that all photoproducts observed still maintain an anthraquinonic structure, some of them resulting from a direct hydroxylation of the initial molecule.

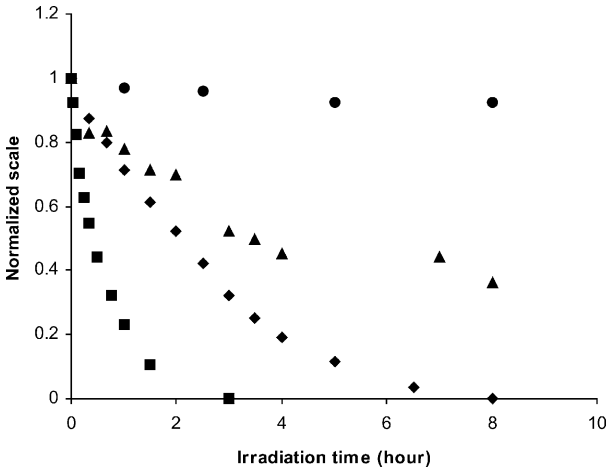

Fig. 5. Photocatalytic degradation of AB25 followed by HPLC–DAD (■) and followed by UV-Vis spectrometry (◆). For both experiments a wavelength of analysis of 600 nm was chosen. Photocatalytic degradation of AB25 followed by TOC analysis (▲). Photolytic degradation of AB25 followed by HPLC–DAD (●). For all experiments, the photon flux measured by actinometry was 0.4×10^{16} photon s^{-1}.

On the same figure, disappearance of AB25 without TiO_2 is also presented to compare the efficiency of the photocatalytic degradation with that of direct photolysis. As expected, the direct photolysis is much slower than photocatalytic degradation since a half-time of 44 h ($k = 1.59 \times 10^{-2}$ h^{-1}) was obtained. This means that photocatalytic degradation is not in concurrence with direct photolysis.

The mineralization of organic carbon was also followed using TOC disappearance (cf. Fig. 5). After 63 h irradiation (result not shown in this figure because of the scale), 90% of the initial organic carbon was transformed into CO_2, thus implying that other organic compounds are still present in the irradiated solution and confirming the noticeable resistance to the degradation of the dye under study. These findings are in agreement with those concerning the photocatalytic degradation of anthraquinone, where the persistence of various aromatic compounds was reported after long-term irradiation [12,13].

3.2.2. Determination of the kinetic order

The kinetic order of the disappearance of AB25 (determined from HPLC measurements) was determined using tangential method. For that, a series of experiments were carried out at different initial concentrations under a constant photonic flux (4.0×10^{15} photons s^{-1}).

The photocatalytic degradation rate r of the AB25 can be expressed as a function of concentration at the adsorption

Table 3
First intermediates tentatively identified by HPLC–MS

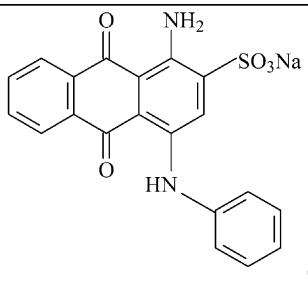 (AB25)	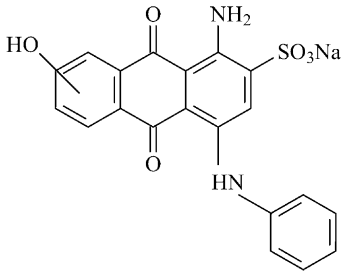
ES^- : 393 $[M\text{-}Na]^-$	ES^- : 409 $[M\text{-}Na]^-$
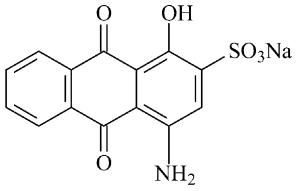	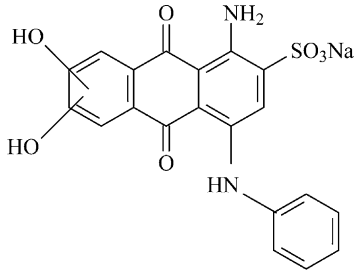
ES^- : 318 $[M\text{-}Na]^-$	ES^- : 425 $[M\text{-}Na]^-$
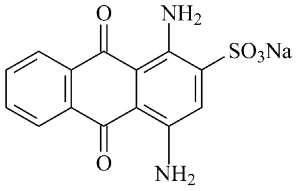	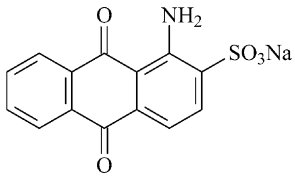
ES^- : 317 $[M\text{-}Na]^-$	ES^- : 302 $[M\text{-}Na]^-$

equilibrium according to:

$$r = \frac{-\mathrm{d}C}{\mathrm{d}t} = k_{ap} C_{eq} \alpha \quad (6)$$

where k_{ap} is the apparent rate constant. The log–log plot of $r = f(C_{eq})$ gives a straight line ($\log r = \log k_{ap} + \alpha \log C_{eq}$) of which slope is equal to the kinetic order.

Fig. 6 shows that α is equal to unity in line with an apparent first-order kinetic law, expected in diluted solutions [6–7].

.

3.3. Influence of the concentration of catalyst and of the photonic flux

In slurry photocatalytic process, the mass m of catalyst can play an important role that can affect the degradation rate. Fig. 7 shows the variation of the rate constant as a function of concentration of catalyst. As can be seen from Fig. 6, the rate constant increases proportionally to the concentration of catalyst and levels off for values close to ca. 2.6 g L^{-1}. Above this value, the rate constant becomes independent of the concentration. Such a value which depends on the nature of the compounds and on the photoreactor geometry is in full agreement with the other ones reported in literature for TiO_2 Degussa-P25, which range from 0.1 to 5.0 g L^{-1} [14–18]. This phenomenon may be explained both by a screening effect of excess particles which masks part of the photosensitive surface and by the scattering of the light which reduces the amount of photons which have

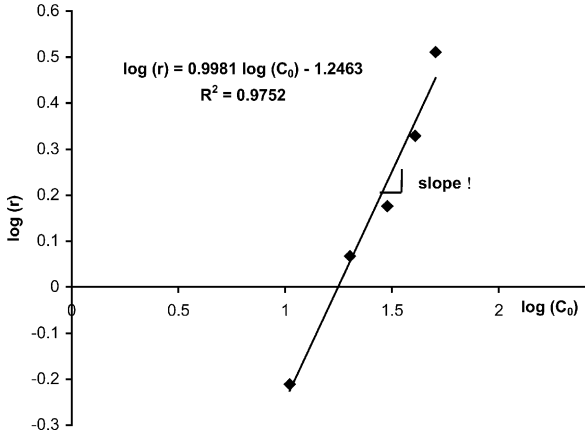

Fig. 6. Log−log of initial rate of photocatalytic degradation of AB25 as a function of the initial concentration.

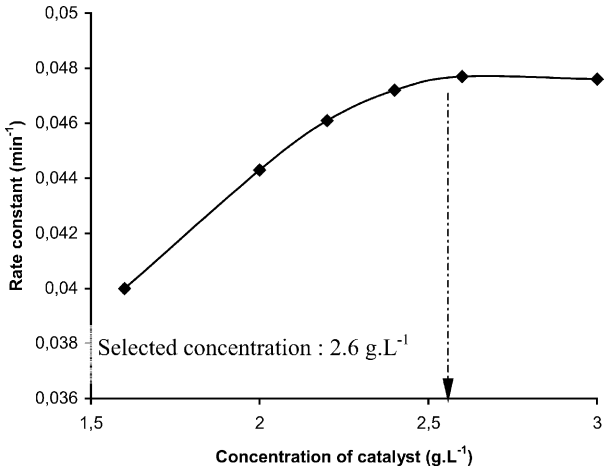

Fig. 7. Variation of the rate constant as a function of concentration of catalyst.

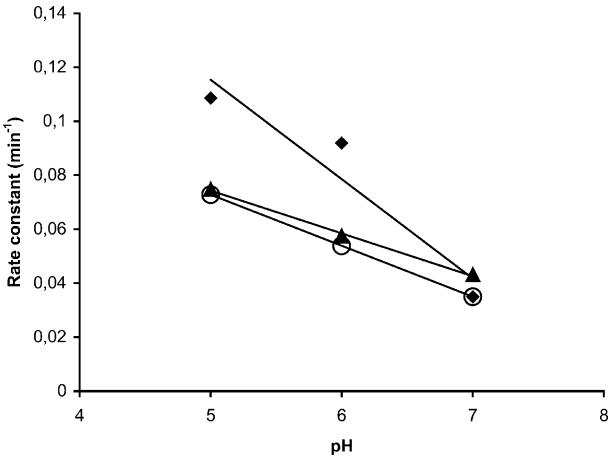

Fig. 9. Evolution of the rate constant as a function of pH for different temperatures (◆ , $T = 20\,^{\circ}C$; ▲, $T = 40\,^{\circ}C$; ○, $T = 60\,^{\circ}C$).

to be absorbed by the catalyst. In the following sections, a TiO_2 concentration of $2.6\,g\,L^{-1}$ was used, unless otherwise stated.

Fig. 8 presents the variation of the rate constant of degradation as a function of the photonic flux. The curve shows that for photonic fluxes ca. $\leq 8.0 \times 10^{16}$ photons s^{-1}, the rate constant is directly proportional to the photonic flux. This means that the process works in a good photocatalytic regime with most of incident photons efficiently converted into active species that act in the degradation mechanism. However, for higher photonic fluxes the rate constant is no longer proportional to the photon flux. In the literature it is suggested that above a certain value the rate of degradation varies as the square root of the photonic flux [6,7]. This indicates that the process is still photocatalytic but that the electron–hole recombination becomes predominant. As we have only one point above 8.0×10^{16} photons s^{-1}, it is difficult to assert a square root variation. However, since the value of 8.0×10^{16} photons s^{-1} for which a change occurs, is close to those found in the literature [6,19], it can be considered that the curve tends to a square root variation as a function of the photonic flux.

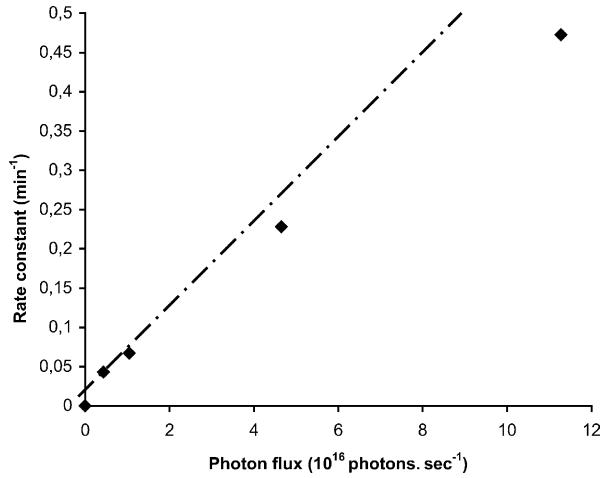

Fig. 8. Variation of the rate constant as a function of photonic flux.

Fig. 9 shows the evolution of rate constant as a function of pH at different temperatures. All the curves show the same trend since, whatever the temperature chosen, a decrease of the rate constant is observed for high pH values. As it was previously shown that at high pH values a decrease of the amount of dye adsorbed on TiO_2 occurred, this result confirms that adsorption plays a major role in the rate of the degradation.

Fig. 9 shows also that the rate constant is higher at 20 °C than at 40 and 60 °C similarly to what have been observed for adsorption.

The apparent activation energy (E_a) at different pH have been calculated from the Arrhenius' equation (Table 2)

$$k = k_0 \exp\left[-\left(\frac{E_a}{RT}\right)\right] \tag{7}$$

The linear transform $\log k = f(1/T)$ gives a straight line whose slope is equal to $-E_a/R$.

Table 2 shows that the activation energy is rather small. By considering the Langmuir–Hinshelwood model to describe the photocatalytic process, the photocatalytic rate r can be expressed by:

$$r = k\theta = k\frac{KC_{eq}}{1 + KC_{eq}} \tag{8}$$

where θ represents the TiO_2 surface coverage as a function of the concentration at the equilibrium C_{eq}.

At low concentrations KC_{eq} can be neglected with respect to 1 and one gets the simplified expression

$$r = kKC_{eq} \tag{9}$$

This equation can also be expressed as a function of temperature by applying the Arrhenius's law to k and the van't

Hoff one to K:

$$r = r_0 \exp\left(\frac{-E_a}{RT}\right) = k_0\, K_0\, C_{eq} \exp\left[\frac{-(E_t + \Delta H)}{RT}\right] \quad (10)$$

Thence

$$E_a = E_t + \Delta H \quad (11)$$

where E_t represents the true activation energy. From this equation, E_t has been calculated and values given in Table 2.

The results in Table 2 imply the following comments. First, the true activation energy E_t is equal to $11.5 \pm 1.5\,\mathrm{kJ\,mol^{-1}}$ in the range of pH investigated. This value is intrinsically very small with respect to those generally observed in heterogeneous catalysis. This underlines the fact that the thermal factor is of secondary importance and that consequently the activation process of the catalyst is essentially a photo-assisted one, as expected in a true photocatalytic system. Secondly, the enthalpy of adsorption of the dye (ΔH) appears as constant at acidic pH and increases above the point of zero charge (pH_{pzc}) of titania. This has to be related again to the ionization state of the surface (cf. Section 3.1). At $pH < pH_{pzc}$, the surface of titania is positively charged (Eq. (4)) and favors AB25 adsorption since this dye is anionic whereas at $pH > pH_{pzc}$ the surface of titania becomes negatively charged (Eq. (3)) and an electrostatic repulsion between TiO_2 and the dye occurs which induces a higher heat of adsorption, i.e. a more negative enthalpy ΔH which decreases from -21 to $-26\,\mathrm{kJ\,mol^{-1}}$. Because of electrostatic repulsion, adsorption requires more energetic sites.

Since the true activation energy E_t remains almost constant around $11.5\,\mathrm{kJ\,mol^{-1}}$ and according to the relationship:

$$E_a = E_t + \Delta H \quad (12)$$

the apparent activation energy E_a increases with ΔH at increasing pH's.

Actually what is the influence of pH upon the kinetics of AB25 degradation?

It is yet known that increasing pH increases ΔH. The direct influence of pH upon kinetics should concern the rate limiting step and the resulting reaction rate can be formally written as:

$$r = f(C, \mathrm{pH}) = f'(C, [H^+]) = k'C[H^+]^n \quad (13)$$

where n is the kinetic partial order with respect to proton concentration. It can be determined from the slope of the log–log plot of $r = f([H^+])$ if

$$r = k'C[H^+]^n \text{ then } \log r = \log k' + \log C + n \log[H^+] = \log k' + \log C - n\mathrm{pH} \quad (14)$$

A value of $n = 0.2$ was found ($T = 20\,^\circ\mathrm{C}$). This value implies the following comments. In absolute value, this fractional value is small, which means that protons do not intervene predominantly in the rate-determining step which is mainly concerned by the attack of the dye molecule by $OH^\bullet$ radicals formed by the following reactions:

$$TiO_2 + h\nu \rightarrow e^- + h^+ \quad (15)$$

$$(H_2O \rightleftarrows H^+ + OH^-) + h^+ \rightarrow H^+ + OH^\bullet \quad (16)$$

$$OH^\bullet + \mathrm{Dye} \rightarrow H_2O + I_1^\bullet \rightarrow \cdots \quad (17)$$

where $I_1^\bullet$ is the first radical intermediate.

However, the order $+0.2$ is substantially more important that values found equal to 0.06 for other dyes [11]. This means that presently, pH is specially influent upon adsorption of AB25 and correlatively and, to a lesser extent, upon the overall kinetics. The positive sign of n ($+0.2$) confirms the favorable degradation of AB25 at acidic pH's as already observed for orange G, another anionic dye.

4. Conclusion

The photocatalytic degradation of AB25 in aqueous solution was studied using TiO_2 Degussa P-25 as a semiconductor catalyst. Adsorption plays an essential role in the degradability of the dye. The effect of TiO_2 concentration on dye degradation was also examined as well as the influence of the photonic flux on the rate constant. By comparing the rate of disappearance of AB25 (followed by HPLC–DAD) with that of the bleaching of the solution (followed by UV-Vis spectrometry), it was put in evidence that some of the intermediate products are also colored. This result was confirmed using HPLC–DAD and HPLC–MS analysis. This study confirms that photocatalysis is suitable not only for decolorizing colored aqueous effluents but also fortunately degrading the dyes and its degradation intermediates to innocuous mineral products (CO_2, H_2O, SO_4^{2-}, etc).

Acknowledgements

This work was supported by Région Rhone-Alpes in the frame of MIRA projects and CMCU (Franco-Tunisian P2R project).

References

[1] M. Schiavello (Ed.), Photocatalysis and Environment: Trends and Applications, NATO ASI Series C, vol. 238, Kluwer Academic Publishers, London, 1987.
[2] D.F. Ollis, H. Al-Ekabi (Eds.), Photocatalytic Purification and Treatment of Water and Air, Elsevier, Amsterdam, 1993.
[3] O. Legrini, E. Oliveros, A. Braun, Chem. Rev. 93 (1993) 671–698.
[4] D. Bahnemann, J. Cunningham, M.A. Fox, E. Pelliziti, P. Pichat, N. Serpone, in: G.R. Zepp, D.G. Crosby (Eds.), Aquatic and Surface Photochemistry, Lewis, Boca Raton, FL, 1994.
[5] D.M. Blake, Bibliography of work on the photocatalytic removal of hazardous compounds from water and air, NREL/TP-430-22197, National Renewable Energy Laboratory, Golden Co., 1997, 1999.

[6] J.M. Herrmann, Catal. Today 53 (1999) 115–129.
[7] J.M. Herrmann, in: F. Jansen, R.A. van Santen (Eds.), Water Treatment by Heterogeneous Photocatalysis in Environmental Catalysis, Catalysis Science Series, vol. 1, Imperial College Press, London, 1999, Chapter 9, pp. 171–194.
[8] E. Pelizzetti, E. Minero, C. Pramauro, in: H.I. Lasa, G. Dogu, A. Ravella (Eds.), Chemical Reactor Technology for Environmentally Safe Reactors and Products, Kluwer Academic Publishers, Dordrecht, The Netherlands, 1993, p. 77.
[9] H.P. Boehm, Adv. Catal. 16 (1966) 179–274.
[10] J. Augustynski, Struct. Bond. 69 (1988) 1–61.
[11] H. Laccheb, E. Puzenat, A. Houas, M. Ksibi, E. Alaloui, C. Guillard, J.M. Herrmann, Appl. Catal. B: Environ. 39 (2002) 75–90.
[12] J. Theurich, D.W. Bahnemann, R. Vogel, F.E. Ehamed, G. Alhakimi, I. Rajab, Res. Chem. Intermed. 23 (1997) 247.
[13] A.B. Prevot, C. Baiocchi, M.C. Brussino, E. Pramauro, P. Savarino, V. Augugliaro, G. Marci, L. Palmisano, Environ. Sci. Technol. 35 (2001) 971–976.
[14] D. Chen, Q.A.K. Ray, Appl. Catal. B: Environ. 23 (1999) 143.
[15] G. Al-Sayyed, J.C. D'Oliveira, P. Pichat, J. Photochem. Photobiol. A: Chem. 58 (1991) 99.
[16] J.P. Percherancier, R. Chapelon, B. Pouyet, J. Photochem. Photobiol. A: Chem. 87 (1995) 261.
[17] J. Gimenez, D. Curco, M.A. Queral, Catal. Today 54 (1999) 229.
[18] S. Parra, J. Olivero, C. Pulgarin, Appl. Catal. B: Environ. 36 (2002) 75.
[19] E. Vulliet, C. Emmelin, J.M. Chovelon, C. Guillard, J.M. Herrmann, Appl. Catal. B: Environ. 38 (2002) 127.